Title: The fastest growing and most destructive fires in the U.S. (2001-2020)

Authors: Jennifer K. Balch[1,2*], Virginia Iglesias[1,3†], Adam L. Mahood[4†], Maxwell C. Cook[2,3], Cibele Amaral[1,3], Amy DeCastro[5], Stefan Leyk[2], Tyler L. McIntosh[3], R. Chelsea Nagy[1,3], Lise St. Denis[3], Ty Tuff[1,3], Erick Verleye[1,3], A. Park Williams[6], Crystal A. Kolden[7]

Affiliations:

[1]Environmental Data Science Innovation and Inclusion Lab (ESIIL), University of Colorado Boulder; Boulder, CO, United States

[2]Department of Geography, University of Colorado Boulder; Boulder, United States

[3]Earth Lab, Cooperative Institute for Research in Environmental Sciences (CIRES), University of Colorado Boulder; Boulder, United States

[4]Water Resources, Agriculture Research Service, United States Department of Agriculture; Fort Collins, United States

[5]Research Applications Laboratory, National Center for Atmospheric Research; Boulder, United States

[6]Department of Geography, University of California Los Angeles; Los Angeles, United States

[7]University of California Merced, Management of Complex Systems Department, School of Engineering; Merced, United States

*Corresponding author. Email: Jennifer.Balch@colorado.edu

†These authors contributed equally to this work.

Abstract: The most destructive and deadly wildfires in U.S. history were also fast. Using satellite data, we analyzed the daily growth rates of over 60,000 fires from 2001-2020 across the contiguous U.S. Nearly half of U.S. ecoregions experienced destructive "fast fires" that grew over 1,620 hectares in one day. These accounted for 78% of structures destroyed and 61% of suppression costs ($18.9 billion). From 2001-2020, the average peak daily growth rate for these fires more than doubled (+249%, relative to 2001) in the western U.S. Nearly three million structures were within four kilometers of a fast fire during this period across the U.S. Given recent devastating wildfires, understanding fast fires is crucial for improving firefighting strategies and community preparedness.

One Sentence Summary: Speed, not size, is the key factor making wildfires deadly and destructive, and they are getting faster.

Main Text: Some of the most deadly and destructive wildfires in contemporary U.S. history have occurred in recent years, with most having the common characteristic of extremely rapid growth. The 2018 Camp fire in California burned over 21,000 ha the day it started, killing 85 people and destroying more than 16,000 homes. The 2021 Marshall fire, the most destructive wildfire in Colorado history, was driven by winds over 100 mph; it traveled 3 miles within the hour it started and burned more than a thousand homes. The 2023 Lahaina fire killed 101 people and destroyed more than 2,200 structures when a small brush fire escaped containment and burned through the town to the shore in two hours. The modern era of ‘megafires’ is often

defined based on wildfire size (*1*), but should be defined based on how fast fires grow and their consequent societal impacts. Fire speed fundamentally dictates the deadly and destructive impact of 'megafires,' rendering the prevailing paradigm that defines them by size inadequate. While big fires change air quality, ecosystems, and carbon dynamics (*2*), fire speed matters more for infrastructure risk and evacuation planning (*3*).

The scientific community has explored trends in extreme fire size (*4, 5*) and burn severity (*6*), and has documented increasing burned area across the western U.S. (*7*). Further, we know that fast fires occur when it is hot, dry and windy, but relatively little research exists about when and why they occur across regional or national scales. Most area burned in extremely large events is from the growth on a single day, which is driven by extreme fire weather, and is predicted to more than double with 2°C warming (*8–10*). Humans also ignite fires in areas with lower tree cover, closer to structures (*3*), and during times with more extreme fire weather (*11*), resulting in more destructive fires (*12*). Recent observational evidence is corroborated by empirical models (*13*) that derive relationships to predict fire growth (*14*), as well as drive landscape fire simulations for individual events (*15, 16*). Such fire behavior models inform wildfire risk models which suggest that the most deadly and damaging wildfires are also some of the fastest (*17, 18*). How fast fires burn also affects burn severity, spatial complexity (*19, 20*), and synchronicity (*21*). Yet, we do not know the patterns, drivers, and consequences of fast fires on a national scale.

Fire suppression policies, logging, the proliferation of invasive species, climate change, and anthropogenic ignition patterns have fundamentally altered the fire-evolved landscapes of post-colonial America (*22–28*). Moreover, the expansion of the urban footprint (*29*) has placed tens of millions of homes squarely into this contemporary fuel matrix, termed the wildland-urban interface (WUI) (*30*). The rapid expansion of this footprint has occurred largely without regard for wildfire risk, either through building policies or comprehensive community planning (*31*). As a result, nearly 60 million homes in the U.S. were threatened by a wildfire between 1992 and 2015 (*3*), a number that has likely increased substantially in the intervening years due to record fires in California, Oregon, and Colorado. Wildfire risk models currently used at a national scale are based on probability of occurrence and area burned, intensity, or severity (*21, 32–35*), rather than how fast wildfires could move. The lack of attention on fire growth is a critical risk assessment gap, particularly given the rapid expansion of the WUI into areas with the greatest probability of wildfire (*36, 37*) and the mechanisms by which most homes burn. We know that the primary mechanism for home ignition is firebrands propelled ahead of the flaming front that land on flammable materials attached to, on, or inside the structure and ultimately consume it (*38*). Firefighters can extinguish these building ignitions during slower fires or when structure ignition is mitigated (*39*), but during fast-moving events they are often overwhelmed by the higher number of homes catching fire simultaneously and the need to focus on life safety and evacuations, e.g., during the 2018 Camp Fire (*17*).

Our lack of understanding is linked to our lack of national data on fire growth rates (FGR) across events. Recent data on individual fire events and how they progressed, coupled with fine-grained settlement data, enable us to explore how fast fires move at a national scale and how that affects residential exposure. We developed a Fire Event Delineation (FIRED) perimeter dataset for over 60,000 fire events (*40*). This dataset is derived from daily burn date estimations from the MODIS burned area product (*41*), enabling calculation and investigation of daily fire growth rate. FGR derived from satellite-detected burned area on a daily basis is different from, but related to, how fast a burning fireline moves on the ground. Settlement data have also become available to

measure trends of development over long time periods at fine resolution (*29*). The Historical Settlement Data Compilation of the U.S. (HISDAC-US) (*42, 43*), which is derived from over 200 million property and housing records, allows us to estimate nearby exposure to wildfires (up to 4 km away). Government records during suppression activities (ICS-209-PLUS) enable us to further explore the societal consequences of wildfires by providing documentation on how many structures were damaged or destroyed on a daily basis during fire events (*25, 44*). The aggregation of ICS-209 reports provides the best available information on the high costs of U.S. wildfires at a national scale. Importantly, the combination of these latter two datasets, HISDAC-US on the spatio-temporal distribution of residential structures and the ICS-209-PLUS on actual structure loss, allows us to explore both potential exposure and documented impact.

Given the critical need to understand fast-moving wildfires and the tens of millions of homes that stand in their paths, we analyzed fires in the context of their speed and damage to homes. We: i) documented the fastest growing fires in the U.S. (2001-2020), exploring the maximum single-day FGR across an event, hereafter maximum FGR, ii) related maximum FGR with structure loss (i.e., damaged or destroyed) to provide a societally-relevant threshold for defining fast fires (maximum FGR > 1,620 ha/day), and iii) explored the trends in maximum FGR and how many total structures, and specifically residences, were exposed to fast fires over the past two decades.

Fire growth rates in the contiguous United States

Fire growth rates were highly variable across all events (N = 60,012), with fires growing at an average rate of 255 ha/day. Maximum FGR ranged from 21-214,200 ha/day, often multiple orders of magnitude greater than the mean FGR across the entire event (Table S1). Fires at the maximum FGR accounted for over a third (38%) of the area burned across the U.S. (Table S2), and more than 70% in some land cover types in certain ecoregions (e.g., shrublands in the Great Plains; Table S2). The maximum FGR is very strongly associated with final fire size across land cover types (Fig. S1), with the log-log relationship suggesting that it follows a power law distribution (adjusted $R^2 = 0.97$). The importance of this is that extreme fire weather on individual days is driving fire growth and has consequences for suppression efforts (*45*). Further, more than 90% of events last no longer than 20 days (Fig. S2A), and 83% of events reach their maximum growth rate within five days, across all ecoregions (Fig. S2B). In addition, there are distinct temporal and spatial characteristics across different vegetation types (e.g., grassland fires burn large areas within a few days while broadleaf forests sustain fire growth for longer periods of time; Fig. S3). Many modeling efforts at regional to national scales model fire activity at monthly to yearly timescales (*4, 46*). These results highlight the need for regional models based on fire behavior that use predictors at daily to hourly time scales, rather than burned area estimations based on topography and spatiotemporally coarse climate data. This is particularly important in the context of modeling the occurrence of extreme meteorological events and their ability to drive rapid fire growth (*20*). Such models exist (*13-15*) and are being further advanced (*33*) but it remains to be tested whether they can replicate the remotely-sensed spread rates in extreme events as reported here. We also found that mean and maximum FGR vary by land cover and ecoregion, with the fastest growing fires typically in the grasslands and savannas of arid ecoregions (Table S3). The 10 fastest fires were in grassland-dominated vegetation which highlights the role of fine, flashy fuels and low wind friction (Table 1 and Table S4). Three highlighted wildfires show how fast fires can grow within the first few days (Fig. 1).

Fast fires are also the most destructive and deadly ones

While there has been substantial focus on megafires defined primarily by their size (*47*), we delineate a critical physical metric that links directly with impact: maximum daily fire growth rate. Treating wildfires as social-environmental extremes (*48*) and defining a subset of events based on both their physical behavior and destructive impact advances our understanding and ability to prepare for such events (*49*). Fires growing faster than 1,620 ha on any single day damage or destroy a large number of structures (Fig. 2). Regression tree analysis (residual mean deviance = 2.39) indicates that one of the best predictors of whether or not a large number of structures were damaged or destroyed across the entire event was whether the maximum FGR exceeded this threshold of 1,620 ha (Supplemental Materials and Methods). Importantly, there is an association between the day of maximum daily growth and the day structures were reported as impacted (Fig. S4). This speed corresponds to the 97th percentile of maximum daily fire growth registered between 2001 and 2020, representing 1,616 events out of 60,012 total events and 60.1% of the burned area in the FIRED record. We, therefore, define "fast fires" as events that grow more than 1,620 ha on a single day (i.e. maximum FGR > 1,620 ha/day). These fast fires represent only 2.7% of all events, yet they account for 89% of the total structures damaged or destroyed. It is important to note that this is a nationwide threshold and reflects if there was any structure loss at all. Of the fires that damaged or destroyed more than 100 structures (N = 71), their average maximum daily growth was 8,569 ha per day (median = 4,916 ha per day). Moreover, there are important differences across states (Table S5). For example, California has by far the highest structure loss compared to other states (N = 66,715 structures damaged or destroyed) and exhibits a fast fire threshold of 2,870 ha/day.

Our results document that 58 of the 85 level 3 ecoregions in the contiguous U.S. experienced more than one fast growing fire between 2001 and 2020 (Fig. S5), representing an area of ~3,780,000 square-kilometers or 49% of CONUS land area. According to the ICS-209-PLUS fire suppression records (2001-2020); (*44*), fast fires threatened 1,780,476 structures (67% of total threatened) and resulted in $18.9 billion of suppression expenditures (61% of total). Moreover, 80,700 structures were destroyed (78% of total destroyed), and 57,883 were damaged (82% of total damaged) across this time-period during fast fire events. This subset of fires represents a significant impact to society, including accounting for 337 fatalities (66% of total) and 5,623 injuries (43% of total).

From 2001-2020, fast fires grew even faster across much of the western U.S.

For all fires, mean FGR significantly increased in 38 and maximum FGR significantly increased in 20 of the 84 level III ecoregions (mainly in the western U.S.). Mean FGR significantly decreased in 16 and maximum FGR significantly decreased in 9 of the ecoregions (mainly in the northeast; Fig. 3 and Fig. S6). Importantly, most of California's ecoregions and coastal Oregon and Washington exhibited an increase in fire growth rate over this period. Most pronounced were the increases in event-level spread and daily growth rates in mediterranean California, with an increase of 300 ha/day in maximum daily growth in Southern California Mountains (Theil-Sen Coefficient = 15.0 ha/day/year; Table S6). Across ecoregions in the state of California, the average maximum FGR increased by 4.2 ha/day/year (± 0.4, s.e.), or approximately 80 ha/day across the 20-year record (Table S7). The Snake River Plain and Columbia Plateau of the North American Desert ecoregion also saw a substantial increase of more than 278 ha/day in maximum daily growth (Theil-Sen Coefficient = 13.9 ha/day/year; Table S6). Across ecoregions in 11 western states, the mean of the maximum FGR increased by 2.1 ha/day/year (± 0.1, s.e.), or approximately 40 ha/day across the 20-year record (Table S7). Based on these trends, fires grew 249% faster (based on maximum daily FGR) across the West by the end of the 20-year record

(Table S8). In California, fires grew 398% faster (based on maximum FGR) by the end of the 20-year record (Table S8). (These percentage increases in California and the western U.S. represent the mean of the maximum FGR in 2020 as a percentage of mean maximum fire growth rate in 2001. See Supplemental Methods.) Across the western U.S. this trend in growth has been accompanied by an increase in annual burned area near built-up areas (< 1 km from a residential structure) of 323% since 2001 (Fig. S7).

Using the HISDAC-US Historical Built-up Property Records (BUPR) (*43*), we estimated that 184,917 properties were exposed directly to fast fires (e.g. within the fire perimeter), 722,017 structures were within one km of fast fire perimeters, and 2,948,501 structures were within four km of fast fire perimeters (Fig. 4 and Fig. S8). Firebrands have ignited WUI materials several kilometers from the main fire (*39*), thus putting structures within this proximity at some risk of loss.

Fire speed matters

Remarkable wildfire events should be defined based on their speed, not just their size. Here we provide a first look at understanding national patterns and trends (2001-2020) in fire growth rate (ha/day) using a satellite-derived metric (*50*). There are two major implications of our work: we define 'fast fires' and we demonstrate that fires are getting faster, particularly in the western U.S.

First, we delineate a new class of the fastest growing and most destructive fires, or 'fast fires.' This class is akin to 'mega-fires,' but is defined based on a maximum daily growth rate of more than 1,620 ha/day where we document the majority of structures destroyed (78%) and suppression costs (61%). A major advance is that this class of 'fast fires' is defined by both the physical behavior and societal impact, representing coupled social-environmental extremes (*48*). We also demonstrate that there is a strong relationship between growth rate and burned area (Fig. S1); importantly, growth is the fundamental mechanism driving final event size. Current national fire risk models and planning efforts tend to focus on fire probability, intensity, or area burned (*50*), rather than fire speed and consequent settlement exposure or potential damage. Fast fires matter for life safety and structure impacts; large fires matter more for ecosystems and generate significant smoke. The speed of a fire determines first whether firefighters are more focused on evacuation than home protection (*17*), and second how effectively they can extinguish burning firebrands and new ignitions on structures before the home becomes fully involved (*38, 39*). Additionally, we quantify that the fastest growing fires are in grassland systems where more homes have been destroyed, relative to forest wildfires (*51*)—highlighting the need to rethink grassland fire management strategies.

Second, we document that fires are growing significantly faster across nearly half of the contiguous U.S. land area—and 2.5 times faster across the western U.S. in just 20 years. Increasing speed will challenge emergency response, evacuation plans, and community preparedness (*52*). Incident command reports indicate that at least 925 emergency evacuation orders affected over 1.5 million households between 2001-2020 (*44*); approximately half of these were within a kilometer of a fast fire (Fig. 4). Wildfire-related emergency evacuation success will be influenced by the density of human settlements, road access (*53*), and efficient use of early warning systems and information delivery to impacted communities (*54*)—all of which will be compromised by faster-moving fires. With maximum daily growth occurring within the first five days after ignition for 83% of all events (Fig. S2B), we also need to focus on proactive measures that slow fires down or promote fire resilience of the built environment. We need to implement building codes that incentivize use of fire-resistant materials (*55*), harden existing

homes and remove flammable materials adjacent to structures (*56*), and preemptively plan for evacuation. Fuel mitigation efforts that will slow fires down include, for example, strategic wildland fuel breaks in the expected path of a fire and re-thinking the constellation of proximate, flammable homes in new developments. Future research efforts will help to better understand the hourly progression of blow-ups from higher resolution satellite sensors and how effective fire suppression teams may already be at slowing wildfires.

Fires may be growing faster due to warming trends, vegetation transitions to more flammable fuels, or the co-occurrence of high winds with increasing human-related ignitions. Climate-driven increases in burned area have been well documented in the U.S. (*57*), as well as an observed tripling of fire frequency in the 2000s relative to the prior two decades (*21*). Many fast fires occur during downslope wind events coincident with anomalously dry autumn conditions, which increased in both frequency (25%) and the area they burn (140%) from 1992-2020 (*59*). Juang et al. (2022) found that the increase in western U.S. forest-fire area since the mid-1980s was driven almost exclusively by increasing sizes of the largest forest fires (*59*). The mechanism is a function of geometric growth: larger fires tend to grow faster than smaller fires because longer firelines have greater potential for spread. It is also known that invasive grasses can drive increases in size (*23*), occurrence, and frequency (*24*). As grass-fueled fires are some of the fastest (Table S3), it may then follow that where vegetation transitions have occurred, e.g., from forest or shrubland to invasive grassland (*60*), fire speed may have also increased. Further, we know that there is a relationship between human ignitions and higher winds (*11, 61*), as lightning generally does not occur under high wind conditions due to the constraints surrounding their associated storms (*61*). Across the U.S. there has been a steady increase (9%) in the percent of wildfires started by human ignitions since 1992 (*62*). It has yet to be tested whether the co-occurrence of windy conditions and human-related ignitions, such as downed power lines, is increasing. People start nearly all the wildfires that threaten our homes (*3*), making understanding of the ignition, climatic, and fuel drivers of fast fires an important area of future work.

The number of fast fire events that have destroyed more than 1,000 homes in just the last five years is alarming (*63*), and may be an expectation in coming years. Fast fires overall accounted for 88% of residential structures destroyed in the U.S. (2001-2020). With warming temperatures increasing the likelihood of wildfires across the U.S. (*64*), we would expect to see more fast events in the future. Given devastating and fast-moving wildfires, such as the Camp wildfire in California, the Marshall wildfire in Colorado, or the Lahaina wildfire in Hawaii, it is critical that we plan for the increasing pace of wildfires.

References and Notes

1. F. Tedim, V. Leone, M. Amraoui, C. Bouillon, M. Coughlan, G. Delogu, P. Fernandes, C. Ferreira, S. McCaffrey, T. McGee, J. Parente, D. Paton, M. Pereira, L. Ribeiro, D. Viegas, G. Xanthopoulos, Defining Extreme Wildfire Events: Difficulties, Challenges, and Impacts. Fire 1, 9 (2018).

2. F. H. Johnston, N. Borchers-Arriagada, G. G. Morgan, B. Jalaludin, A. J. Palmer, G. J. Williamson, D. M. J. S. Bowman, Unprecedented health costs of smoke-related PM2.5 from the 2019–20 Australian megafires. Nat. Sustain. 4, 42–47 (2021).

3. N. Mietkiewicz, J. K. Balch, T. Schoennagel, S. Leyk, L. A. St. Denis, B. A. Bradley, In the Line of Fire: Consequences of Human-Ignited Wildfires to Homes in the U.S. (1992–2015). Fire 3, 50 (2020).

4. M. B. Joseph, M. W. Rossi, N. P. Mietkiewicz, A. L. Mahood, M. E. Cattau, R. C. Nagy, V. Iglesias, J. T. Abatzoglou, J. K. Balch, Spatiotemporal prediction of wildfire size extremes with Bayesian finite sample maxima. Ecol. Appl. 29, 1266–1281 (2019).

5. R. C. Nagy, E. Fusco, B. Bradley, J. T. Abatzoglou, J. Balch, Human-Related Ignitions Increase the Number of Large Wildfires across U.S. Ecoregions. Fire 1, 4 (2018).

6. S. A. Parks, J. T. Abatzoglou, Warmer and Drier Fire Seasons Contribute to Increases in Area Burned at High Severity in Western US Forests From 1985 to 2017. Geophys. Res. Lett. 47 (2020).

7. J. Buch, A. P. Williams, C. S. Juang, W. D. Hansen, P. Gentine, SMLFire1.0: a stochastic machine learning (SML) model for wildfire activity in the western United States. Geosci. Model Dev. 16, 3407–3433 (2023).

8. P. T. Brown, H. Hanley, A. Mahesh, C. Reed, S. J. Strenfel, S. J. Davis, A. K. Kochanski, C. B. Clements, Climate warming increases extreme daily wildfire growth risk in California. Nature 621, 760–766 (2023).

9. J. D. Coop, S. A. Parks, C. S. Stevens-Rumann, S. M. Ritter, C. M. Hoffman, Extreme fire spread events and area burned under recent and future climate in the western USA. Glob. Ecol. Biogeogr. 31, 1949–1959 (2022).

10. B. E. Potter, D. McEvoy, Weather Factors Associated with Extremely Large Fires and Fire Growth Days. Earth Interact. 25, 160–176 (2021).

11. S. Hantson, N. Andela, M. L. Goulden, J. T. Randerson, Human-ignited fires result in more extreme fire behavior and ecosystem impacts. Nat. Commun. 13, 2717 (2022).

12. A. D. Syphard, J. E. Keeley, M. Gough, M. Lazarz, J. Rogan, What Makes Wildfires Destructive in California? Fire 5, 133 (2022).

13. R. C. Rothermel, A Mathematical Model for Predicting Fire Spread in Wildland Fuels (Intermountain Forest & Range Experiment Station, Forest Service, US …, 1972)vol. 115.

14. P. L. Andrews, BEHAVE: fire behavior prediction and fuel modeling system. USDA For. Serv. Gen. Tech. Rep. INT 194 (1986).

15. A. L. Sullivan, Wildland surface fire spread modelling, 1990 - 2007. 1: Physical and quasi-physical models. Int. J. Wildland Fire 18, 349 (2009).

16. J. L. Coen, Simulation of the Big Elk Fire using coupled atmosphere–fire modeling. Int. J. Wildland Fire 14, 49–59 (2005).

17. A. Maranghides, E. Link, W. “Ruddy” Mell, S. Hawks, M. Wilson, W. Brewer, C. Brown, B. Vihnaneck, W. D. Walton, “A Case Study of the Camp Fire – Fire Progression Timeline” (NIST TN 2135, National Institute of Standards and Technology, Gaithersburg, MD, 2021); https://doi.org/10.6028/NIST.TN.2135.

18. C. C. Wilson, Fatal and Near-Fatal Forest Fires The Common Denominators. Int. Fire Chief 43, 9–10, 12–15 (1977).

19. D. A. Falk, E. K. Heyerdahl, P. M. Brown, C. Farris, P. Z. Fulé, D. McKenzie, T. W. Swetnam, A. H. Taylor, M. L. Van Horne, Multi-scale controls of historical forest-fire regimes: new insights from fire-scar networks. Front. Ecol. Environ. 9, 446–454 (2011).
20. X. Wang, T. Swystun, J. Oliver, M. D. Flannigan, One extreme fire weather event determines the extent and frequency of wildland fires. Environ. Res. Lett. 16, 114031 (2021).
21. V. Iglesias, J. K. Balch, W. R. Travis, U.S. fires became larger, more frequent, and more widespread in the 2000s. Sci. Adv. 8, eabc0020 (2022).
22. J. K. Balch, B. A. Bradley, J. T. Abatzoglou, R. C. Nagy, E. J. Fusco, A. L. Mahood, Human-started wildfires expand the fire niche across the United States. Proc. Natl. Acad. Sci. 114, 2946–2951 (2017).
23. J. K. Balch, B. A. Bradley, C. M. D'Antonio, J. Gómez-Dans, Introduced annual grass increases regional fire activity across the arid western USA (1980-2009). Glob. Change Biol. 19, 173–183 (2013).
24. E. J. Fusco, J. T. Finn, J. K. Balch, R. C. Nagy, B. A. Bradley, Invasive grasses increase fire occurrence and frequency across US ecoregions. Proc. Natl. Acad. Sci. 116, 23594–23599 (2019).
25. P. E. Higuera, M. C. Cook, J. K. Balch, E. N. Stavros, A. L. Mahood, L. A. St. Denis, Shifting social-ecological fire regimes explain increasing structure loss from Western wildfires. PNAS Nexus 2, pgad005 (2023).
26. C. Naficy, A. Sala, E. G. Keeling, J. Graham, T. H. DeLuca, Interactive effects of historical logging and fire exclusion on ponderosa pine forest structure in the northern Rockies. Ecol. Appl. 20, 1851–1864 (2010).
27. S. J. Pyne, Fire in America: A Cultural History of Wildland and Rural Fire (University of Washington Press, Seattle, Pbk. ed., 1997)Cycle of fire.
28. A. P. Williams, J. T. Abatzoglou, Recent Advances and Remaining Uncertainties in Resolving Past and Future Climate Effects on Global Fire Activity. Curr. Clim. Change Rep. 2, 1–14 (2016).
29. S. Leyk, J. H. Uhl, D. S. Connor, A. E. Braswell, N. Mietkiewicz, J. K. Balch, M. Gutmann, Two centuries of settlement and urban development in the United States. Sci. Adv. 6, eaba2937 (2020).
30. S. I. Stewart, V. C. Radeloff, R. B. Hammer, T. J. Hawbaker, Defining the Wildland–Urban Interface. J. For. 105, 201–207 (2007).
31. H. A. Kramer, V. Butsic, M. H. Mockrin, C. Ramirez-Reyes, P. M. Alexandre, V. C. Radeloff, Post-wildfire rebuilding and new development in California indicates minimal adaptation to fire risk. Land Use Policy 107, 105502 (2021).
32. G. K. Dillon, J. P. Menakis, F. fay, Wildland Fire Potential: A Tool for Assessing Wildfire Risk and Fuels Management Needs. USDA For. Serv. Proc. RMRS-P-73, 17 (2015).
33. M. A. Finney, C. W. McHugh, I. C. Grenfell, K. L. Riley, K. C. Short, A simulation of probabilistic wildfire risk components for the continental United States. Stoch. Environ. Res. Risk Assess. 25, 973–1000 (2011).

34. J. R. Haas, D. E. Calkin, M. P. Thompson, A national approach for integrating wildfire simulation modeling into Wildland Urban Interface risk assessments within the United States. Landsc. Urban Plan. 119, 44–53 (2013).

35. R. G. Haight, D. T. Cleland, R. B. Hammer, V. C. Radeloff, T. S. Rupp, Assessing Fire Risk in the Wildland-Urban Interface. J. For. October/November, 41–48 (2004).

36. V. C. Radeloff, D. P. Helmers, H. A. Kramer, M. H. Mockrin, P. M. Alexandre, A. Bar-Massada, V. Butsic, T. J. Hawbaker, S. Martinuzzi, A. D. Syphard, S. I. Stewart, Rapid growth of the US wildland-urban interface raises wildfire risk. Proc. Natl. Acad. Sci. 115, 3314–3319 (2018).

37. K. Rao, A. P. Williams, N. S. Diffenbaugh, M. Yebra, A. G. Konings, Plant-water sensitivity regulates wildfire vulnerability. Nat. Ecol. Evol., doi: 10.1038/s41559-021-01654-2 (2022).

38. S. Nazare, I. Leventon, R. Davis, "Ignitibility of structural wood products exposed to embers during wildland fires : a review of literature" (NIST TN 2153, National Institute of Standards and Technology (U.S.), Gaithersburg, MD, 2021); https://doi.org/10.6028/NIST.TN.2153.

39. C. A. Kolden, C. Henson, A Socio-Ecological Approach to Mitigating Wildfire Vulnerability in the Wildland Urban Interface: A Case Study from the 2017 Thomas Fire. Fire 2, 9 (2019).

40. J. K. Balch, L. A. St. Denis, A. L. Mahood, N. P. Mietkiewicz, T. M. Williams, J. McGlinchy, M. C. Cook, FIRED (Fire Events Delineation): An Open, Flexible Algorithm and Database of US Fire Events Derived from the MODIS Burned Area Product (2001–2019). Remote Sens. 12, 3498 (2020).

41. L. Giglio, L. Boschetti, D. P. Roy, M. L. Humber, C. O. Justice, The Collection 6 MODIS burned area mapping algorithm and product. Remote Sens. Environ. 217, 72–85 (2018).

42. S. Leyk, J. H. Uhl, HISDAC-US, historical settlement data compilation for the conterminous United States over 200 years. Sci. Data 5, 180175 (2018).

43. J. H. Uhl, S. Leyk, C. M. McShane, A. E. Braswell, D. S. Connor, D. Balk, Fine-grained, spatiotemporal datasets measuring 200 years of land development in the United States. Earth Syst. Sci. Data 13, 119–153 (2021).

44. L. A. St. Denis, K. C. Short, K. McConnell, M. C. Cook, N. P. Mietkiewicz, M. Buckland, J. K. Balch, All-hazards dataset mined from the US National Incident Management System 1999–2020. Sci. Data 10, 112 (2023).

45. M. Goss, D. L. Swain, J. T. Abatzoglou, A. Sarhadi, C. A. Kolden, A. P. Williams, N. S. Diffenbaugh, Climate change is increasing the likelihood of extreme autumn wildfire conditions across California. Environ. Res. Lett. 15, 094016 (2020).

46. M. A. Moritz, M.-A. Parisien, E. Batllori, M. A. Krawchuk, J. Van Dorn, D. J. Ganz, K. Hayhoe, Climate change and disruptions to global fire activity. Ecosphere 3, art49 (2012).

47. S. L. Stephens, N. Burrows, A. Buyantuyev, R. W. Gray, R. E. Keane, R. Kubian, S. Liu, F. Seijo, L. Shu, K. G. Tolhurst, J. W. van Wagtendonk, Temperate and boreal forest mega-fires: characteristics and challenges. Front. Ecol. Environ. 12, 115–122 (2014).

48. J. K. Balch, V. Iglesias, A. E. Braswell, M. W. Rossi, M. B. Joseph, A. L. Mahood, T. R. Shrum, C. T. White, V. M. Scholl, B. McGuire, C. Karban, M. Buckland, W. R. Travis, Social-Environmental Extremes: Rethinking Extraordinary Events as Outcomes of Interacting Biophysical and Social Systems. Earths Future 8 (2020).

49. M. C. Cook, "Drivers of wildfire-related home loss across the western United States 2001-2018," thesis, University of Colorado (2021).

50. J. H. Scott, M. P. Thompson, D. E. Calkin, "A wildfire risk assessment framework for land and resource management" (General Technical Report General Technical Report RMRS-GTR-315, U.S. Department of Agriculture, Forest Service, Rocky Mountain Research Station, 2013); https://digitalcommons.unl.edu/cgi/viewcontent.cgi?article=1334&context=usdafsfacpub.

51. V. C. Radeloff, M. H. Mockrin, D. Helmers, A. Carlson, T. J. Hawbaker, S. Martinuzzi, F. Schug, P. M. Alexandre, H. A. Kramer, A. M. Pidgeon, Rising wildfire risk to houses in the United States, especially in grasslands and shrublands. Science 382, 702–707 (2023).

52. T. J. Cova, D. Li, L. K. Siebeneck, F. A. Drews, Toward Simulating Dire Wildfire Scenarios. Nat. Hazards Rev. 22, 06021003 (2021).

53. P. E. Dennison, T. J. Cova, M. A. Mortiz, WUIVAC: a wildland-urban interface evacuation trigger model applied in strategic wildfire scenarios. Nat. Hazards 41, 181–199 (2007).

54. E. Kuligowski, Evacuation decision-making and behavior in wildfires: Past research, current challenges and a future research agenda. Fire Saf. J. 120, 103129 (2021).

55. S. L. Quarles, K. Pohl, Building a Wildfire-Resistant Home: Codes and Costs (2018). https://headwaterseconomics.org/wildfire/homes-risk/building-costs-codes.

56. S. L. Quarles, C. Standohar-Alfano, F. Hedayati, D. J. Gorham, Factors influencing ember accumulation near a building. Int. J. Wildland Fire 32, 380–387 (2023).

57. J. T. Abatzoglou, A. P. Williams, Impact of anthropogenic climate change on wildfire across western US forests. Proc. Natl. Acad. Sci. 113, 11770–11775 (2016).

58. J. T. Abatzoglou, C. A. Kolden, A. P. Williams, M. Sadegh, J. K. Balch, A. Hall, Downslope Wind-Driven Fires in the Western United States. Earths Future 11, e2022EF003471 (2023).

59. C. S. Juang, A. P. Williams, J. T. Abatzoglou, J. K. Balch, M. D. Hurteau, M. A. Moritz, Rapid Growth of Large Forest Fires Drives the Exponential Response of Annual Forest-Fire Area to Aridity in the Western United States. Geophys. Res. Lett. 49, e2021GL097131 (2022).

60. A. L. Mahood, J. K. Balch, Repeated fires reduce plant diversity in low-elevation Wyoming big sagebrush ecosystems (1984–2014). Ecosphere 10, e02591 (2019).

61. J. T. Abatzoglou, J. K. Balch, B. A. Bradley, C. A. Kolden, J. T. Abatzoglou, J. K. Balch, B. A. Bradley, C. A. Kolden, Human-related ignitions concurrent with high winds promote large wildfires across the USA. Int. J. Wildland Fire 27, 377–386 (2018).

62. M. E. Cattau, C. Wessman, A. Mahood, J. K. Balch, Anthropogenic and lightning-started fires are becoming larger and more frequent over a longer season length in the U.S.A. Glob. Ecol. Biogeogr. 29, 668–681 (2020).

63. K. Barrett, T. Preston, K. Pohl, P. Hernandez, “Wildfires destroy thousands of structures each year” (Headwaters Economics, 2020); https://headwaterseconomics.org/natural-hazards/structures-destroyed-by-wildfire/.

64. J. J. Stephens, M. B. Joseph, V. Iglesias, T. A. Tuff, A. L. Mahood, I. Rangwala, J. Wolken, J. K. Balch, “Fires of Unusual Size: Future of Extreme and Emerging Wildfires in a Warming United States (2020-2060).” [Preprint] (2023). https://doi.org/10.22541/essoar.170224524.49212451/v1.

65. L. St. Denis, K. Short, K. McConnell, M. Cook, M. Buckland, N. Mietkiewicz, J. Balch, All-hazards dataset mined from the US National Incident Management System 1999-2020 (Dataset), figshare (2023); https://doi.org/10.6084/m9.figshare.19858927.v3.

66. J. Eidenshink, B. Schwind, K. Brewer, Z.-L. Zhu, B. Quayle, S. Howard, A Project for Monitoring Trends in Burn Severity. Fire Ecol. 3, 3–21 (2007).

67. M. Friedl, D. Sulla-Menashe, MCD12C1 MODIS/Terra+Aqua Land Cover Type Yearly L3 Global 0.05Deg CMG V006, EarthData (2015); https://doi.org/10.5067/MODIS/MCD12C1.006.

68. Commission for Environmental Cooperation, Ecological regions of North America: toward a common perspective. (2006).

69. J. M. Omernik, G. E. Griffith, Ecoregions of the Conterminous United States: Evolution of a Hierarchical Spatial Framework. Environ. Manage. 54, 1249–1266 (2014).

70. Y. Chen, S. Hantson, N. Andela, S. R. Coffield, C. A. Graff, D. C. Morton, L. E. Ott, E. Foufoula-Georgiou, P. Smyth, M. L. Goulden, J. T. Randerson, California wildfire spread derived using VIIRS satellite observations and an object-based tracking system. Sci. Data 9, 249 (2022).

71. A. DeCastro, “Integrating Remote Sensing, Behavior Modeling, and Machine Learning to Better Understand the Patterns and Drivers of Wildfire,” thesis, University of Colorado Boulder (2022).

72. P. K. Sen, Estimates of the Regression Coefficient Based on Kendall’s Tau. J. Am. Stat. Assoc. 63, 1379–1389 (1968).

73. X. Wang, Q. Yu, Unbiasedness of the Theil–Sen estimator. J. Nonparametric Stat. 17, 685–695 (2005).

74. L. A. St. Denis, N. P. Mietkiewicz, K. C. Short, M. Buckland, J. K. Balch, All-hazards dataset mined from the US National Incident Management System 1999–2014. Sci. Data 7, 64 (2020).

75. L. Breiman, J. H. Friedman, R. A. Olshen, C. J. Stone, Classification And Regression Trees (Routledge, ed. 1, 1984; https://www.taylorfrancis.com/books/9781351460491).

76. Y. Ahn, S. Leyk, J. H. Uhl, C. M. McShane, An Integrated Multi-Source Dataset for Measuring Settlement Evolution in the United States from 1810 to 2020. Sci. Data 11, 275 (2024).

77. J. H. Uhl, S. Leyk, Uncertainty surfaces accompanying the BUPR, BUPL, and BUA gridded surface series, Harvard Dataverse (2020); https://doi.org/10.7910/DVN/T8H5KF.

78. A. C. Fernandez-Pello, Wildland fire spot ignition by sparks and firebrands. Fire Saf. J. 91, 2–10 (2017).

Acknowledgments: We are grateful to Stephen Pyne, Nathan Mietkiewicz, Michael Koontz, and Johannes Uhl for discussions that informed this effort, as well as two anonymous reviewers for feedback and suggestions that improved the manuscript.

Funding: This study was supported by:

Earth Lab, University of Colorado - Boulder, Grand Challenge and CIRES (JKB, RCN, CA, EV, TT, VI, AM, LS)

National Science Foundation Macrosystems Program grant 2017889 (JKB, TLM)

National Science Foundation CAREER Program grant 1846384 (JKB, TLM)

National Science Foundation HNDS-I Program grant 2121976 (SL, JKB)

Joint Fire Sciences Program grant 21-2-02-29 (JKB, MC)

USDA NIFA grant 2022-67019-36435 (CK)

Gordon and Betty Moore Foundation grants GBMF10763 and GBMF11974 (APW).

Author contributions:

Conceptualization: JKB, ALM, VI, MCC, APW

Methodology: JKB, ALM, VI, MCC, AD

Investigation: JKB, ALM, VI, MCC, RCN, AD, TLM

Visualization: VI, MCC, ALM, TLM, JKB

Data Curation: CA, EV, LS, MCC, JKB

Software: CA, EV, MCC, TT, JKB

Funding acquisition: JKB, RCN

Project administration: JKB, RCN

Supervision: JKB

Writing – original draft: JKB, ALM, VI, MCC, APW, RCN, TT, SL, CK, AD, CA

Writing – review & editing: JKB, ALM, VI, MCC, APW, RCN, TT, TLM, SL, CK, AD, CA

Competing interests: Authors declare that they have no competing interests.

Data and materials availability: All data used in this analysis are publicly available at the following DOIs and URLs. All code necessary to reproduce this analysis is available at https://github.com/viriglesias/fast-fires. The workflow to derive the linked ICS-209+ and FIRED product per (*44*) is available at https://github.com/maxwellCcook/ics209-plus-fired/blob/main/code/R/ics-fired.Rmd. Data access and repositories: All-hazards dataset mined from the US National Incident Management System is hosted on figshare (*65*). Fire Events Delineation (FIRED) CONUS-AK 2001-2022: https://scholar.colorado.edu/concern/datasets/d504rm74m. United States Environmental Protection Agency ecoregions: https://www.epa.gov/eco-research/ecoregions. Monitoring Trends in Burn Severity (MTBS): https://www.mtbs.gov/.

Supplementary Materials

Materials and Methods

Supplementary Text

Figs. S1 to S8

Tables S1 to S8

References (66-78)

Fig 1. Fast fires in the U.S. (A) Locations of all recorded fast fires (max FGR > 1,620 ha, 2001-2020, N = 1,616, in gray) in the contiguous United States (CONUS) with the top 100 fastest fires scaled in color and size by their maximum single-day fire growth in hectares/day. The fastest fires occurred primarily in the western United States and in the southeastern plains (Texas and Oklahoma), but across a wide range of ecoregions and fuel types. **(B-D)** Three examples of the fastest fires on record highlight the daily burned area from the MODIS Burned Area product (MCD64A1), fire perimeters from the Monitoring Trends in Burn Severity (MTBS), and approximate locations of properties within the burned area from the Historical Built-Up Property Records (BUPR) obtained from the HISDAC-US database. **(B)** The Northwest Oklahoma Complex fire in 2018 is the fastest recorded fire in the database with a single day maximum growth of 214,208 ha/day, burning in grasslands; **(C)** the Cold Springs fire in 2020 is part of the destructive Labor Day fires which burned in high winds and together with the Pearl Hill and Whitney fires burned over 165,000 hectares in a matter of days. The Cold Springs fire was the largest of the three and burned almost entirely in a single day (102,198 ha/day); **(D)** the Witch and Poomacha fires in 2003 burned just outside of San Diego, CA, directly exposing over 8,000 properties within days (with more than 76,000 properties within 4 km of the burned area) and destroying 1,680 structures, making it one of the most destructive fast fires in the database.

Fig. 2. Defining fast fires as a function of social-economic impacts. Scatterplot of log-transformed maximum fire growth rate and log-transformed number of structures destroyed, with marginal probability density distributions. The dashed line shows the lower bound of growth of 'fast fires' (1,620 ha/day or above) that were also the most destructive ones. Note that the axes are in log scale and that only fast fires destroyed more than 600 structures.

Fig. 3. Temporal trends in maximum annual fire growth on a given day for events longer than four days per EPA ecoregion level IV (2001-2020). Statistically-significant positive and negative regression coefficients ($p < 0.05$) are depicted in warm and cold colors, respectively. Regression coefficients that were not statistically significant from zero (i.e., no significant trend) are shown in white. Ecoregions without sufficient data for the analysis are indicated in gray.

Fig. 4. Exposure to fast fires (>1,620 ha/day) in 2001-2020. (**A**) Number of fast fires per year. (**B**) Annual area affected by fast fires. (**C**) Trends in the number of structures (based on the BUPR dataset) within the perimeters of ***fast fires*** (black), within 1 km of the perimeters of fast fires (dark gray), and within 4 km of the perimeters of fast fires (light gray).

Incident Name	Year	State	Fire Size (ha)	Max Fire Growth (ha/day)	Duration	Cost ($)	Properties Exposed (4km)	Structures Destroyed	Total Aerial Units	Total Personnel	Dominant Vegetation
NW Oklahoma Complex	2017	OK, KS	315,369	214,208	16	$3,200,000	1,647	151	2	955	Grasslands
Long Draw	2012	OR	225,664	129,911	14	$4,360,000	2	0	49	4,237	Grasslands
Cold Springs Complex	2020	WA	218,969	102,199	33	$11,459,351	4,907	288	34	4,327	Grasslands
Perryton	2017	TX	128,753	100,911	14	NR	97	11	3	235	Grasslands
Anderson Creek	2016	OK, KS	148,819	81,420	19	$1,750,000	1,098	54	20	1,183	Grasslands
Murphy Complex	2007	ID	263,862	70,150	30	$13,000,000	21	3	56	10,443	Grasslands
East Amarillo Complex	2006	TX	367,149	60,770	23	NR	4,821	89	6	702	Grasslands
Martin	2018	NV	176,269	59,246	20	$8,500,000	0	1	97	2,332	Grasslands
Milford Flat	2007	UT	146,922	58,258	16	$5,050,000	112	2	25	4,421	Grasslands
Glass	2008	TX	88,851	57,979	5	NR	1	0	8	56	Grasslands
Buzzard Complex	2014	OR	160,153	50,252	14	$11,062,411	42	4	96	5,265	Grasslands
August Complex	2020	CA	417,898	49,629	68	$115,511,218	196	446	1,153	63,814	Evergreen Needleleaf Forests
Kinyon Road	2012	ID	85,338	47,461	12	$1,625,000	57	0	18	1,361	Grasslands
Soda	2015	ID	115,482	46,474	9	$6,250,000	662	1	69	1,706	Grasslands
Rhea	2018	OK	115,820	44,499	26	$3,707,498	1,669	32	62	941	Grasslands
North Complex	2020	CA	129,069	42,438	52	$112,711,950	4,607	2342	802	63,229	Evergreen Needleleaf Forests
Cedar	2003	CA	110,579	41,408	18	$32,616,213	132,444	2820	626	74,404	Closed Shrublands
Cooper Mtn. Ranch	2011	TX	65,812	39,969	13	$1,194,159	740	0	8	854	Grasslands
LNU Lightning Complex	2020	CA	146,990	39,132	22	$94,646,381	34,344	1479	354	36,601	Grasslands
Witch-Poomacha	2007	CA	80,124	38,639	19	$18,000,000	76,871	1680	2	46,819	Closed Shrublands

Table 1. Top 20 fastest growing fires across the contiguous U.S. (2001-2020). Summary statistics describing the top 20 fastest fires from FIRED linked to their associated incident command system summary report (*44*). The top 20 fastest fires accrued an estimated $398M in suppression costs alone, exposed 264,338 properties (within 4 km of a fire perimeter) and destroyed over 9,000 structures. Of the 20 fastest fires, 16 occurred primarily in grassland vegetation types (>50% grassland in burned area).

Science
AAAS

Supplementary Materials for

The fastest growing and most destructive fires in the U.S. (2001-2020)

Jennifer K. Balch[1,2*], Virginia Iglesias[1,3†], Adam L. Mahood[4†], Maxwell C. Cook[2,3], Cibele Amaral[1,3], Amy DeCastro[5], Stefan Leyk[2], Tyler L. McIntosh[3], R. Chelsea Nagy[1,3], Lise St. Denis[3], Ty Tuff[1,3], Erick Verleye[1,3], A. Park Williams[6], Crystal A. Kolden[7]

Correspondence to: Jennifer.Balch@colorado.edu

This PDF file includes:

Other Supplementary Materials for this manuscript include the following:

Tables S1-S6 (separate files)

Materials and Methods

I. Characterizing fire growth rates for 60,000 events across the contiguous U.S.

We used the Fire Event Delineation algorithm (FIRED) (*40*) to define fire events from which we obtained information on the daily progression of all fires in the U.S. from the MODIS Collection 6 MCD64A1 Burned Area Product for 2001-2020. FIRED is a spatiotemporal flooding algorithm that inputs an area of interest, temporal extent, and spatial and temporal parameters, and uses these inputs to group gridded, daily burned area detections into events. We used spatio-temporal parameters of five 463-m pixels and 11 days based on a Monitoring Trends in Burn Severity (MTBS)-based optimization (*40, 66*). FIRED outputs each event as a single fire perimeter as well as daily progression maps. For each event, and daily subset, the modal International Geosphere-Biosphere Programme (IGBP) land cover classification was extracted from the MOD12c1 product (*67*). In order to minimize the confounding effect of fires that were intentionally started, we excluded croplands. We utilized 60,012 events for these analyses. For each fire event, we calculated the fire growth rate (FGR) for an entire fire event, and the maximum single-day fire growth rate, or maximum FGR. FGR was calculated as the burned area for the entire event divided by the duration, and maximum FGR was the area burned on the day with the largest burned area.

Fire growth rate in the contiguous U.S. is highly variable. To identify areas of fast versus slow fire spread, we overlaid the FIRED data layers with Environmental Protection Agency level IV ecoregions (*68*). These ecoregions reflect spatial differences in geology, landforms, soils, vegetation, climate, land use, wildlife, and hydrology (*69*). For each ecoregion, we calculated the maximum FGR (single day within an event), median FGR (across an event), and mean FGR (across an event).

It is important to note that daily growth rate is not equivalent to the spread rate of an actual fireline, although they are certainly related variables. Daily growth rate is integrated across a burned area pixel (~25 ha, or 250,000 m^2) on an approximate daily basis based on the temporal resolution of the MODIS burned area product (MCD64A1). The MCD64A1 approximates the day of burning based on rapid changes in MODIS surface reflectance and is thus subject to uncertainties based on image quality, availability, and the output of the change detection algorithm (*41*). Work is being done to integrate active fire satellite products to better characterize linear fireline spread on much finer spatial and temporal resolutions (*70*) and to understand how to approximate linear growth from areal growth (*71*).

II. Detecting temporal trends in fire growth rates and event duration (2001-2020)

To identify temporal changes in fire dynamics, we produced a time series of maximum annual FGR (i.e., at one-year timesteps) for each level III ecoregion (*68*). We chose to segment the contiguous U.S. with level III ecoregions, which are coarser than level IV ecoregions, to ensure that most time series had sufficient data points to allow for meaningful trend analysis and detection.

The probabilistic distribution of fire growth rates has a very heavy left tail. To obtain robust temporal trends, we excluded events shorter than five days and ecoregions with less than 10 data points. We then used the Theil-Sen estimator to fit linear models to the time series that satisfied these conditions. By estimating the median of all slopes defined by all pairs of points in a two-dimensional space (*72*), this method provides an unbiased estimate of the regression slope (*73*) and it is less sensitive to outliers. The statistical significance of each trend was assessed with Wilcoxon tests ($p < 0.05$).

We also estimated trends in maximum FGR in California and the 11 western states (Table S7), where most fast fires have taken place (i.e., Washington, Oregon, California, Idaho, Utah, Nevada, Arizona, Montana, Wyoming, Colorado, and New Mexico). To this end, we produced time series of maximum single-day growth for ecoregions within California or the western U.S. boundary and excluded events shorter than five days. We then randomly drew 2,500 bootstrap samples with replacement from the resulting data set and used the Theil-Sen estimator to compute the Kendall-Theil robust line (or Sen's slope). We repeated this procedure 1,000 times. This allowed us to estimate the standard errors of the mean and median regression slope and intercepts.

III. Defining fast fires based on societal impact

Fire impacts depend not only on the physical properties of fire but also on the assets in harm's way. This work operationalizes a definition of fast fires, based on a framework that defines socio-environmental extremes given both their physical characteristics and social consequences (*48*). Defining fast fires required partitioning the continuum of fire speeds into two discrete classes, fast and non-fast. Given that 'fast' is a relative concept, the threshold between these classes is conditioned by the fundamental question of 'fast with respect to what?'. Here, we focus on fires whose spread rates are higher than those that are not likely to have significant societal impact.

To estimate this threshold, we constructed a dataset that combined fire growth rates from FIRED (*40*) and information on the number of structures damaged or destroyed per event obtained from incident command reports, or the ICS-209-PLUS database (*74*), via spatiotemporal overlay. The linked ICS-209 wildfire events and FIRED, the MODIS-derived perimeter product, is published (*44*) and the workflow is available at GitHub here: https://github.com/maxwellCcook/ics209-plus-fired/blob/main/code/R/ics-fired.Rmd. The ICS-209-PLUS dataset includes two products; the incident summary report which aggregates attributes for the entire event, and the daily situation reports which provide the daily snapshot for all attributes, including daily estimates of structures destroyed and threatened. While the ICS-209-PLUS data do not provide structure locations (i.e., addresses, building destruction maps), by comparing daily situation reports to the FIRED maximum daily FGR, we do document that there is an association between the day of maximum daily growth and the day structures were reported as impacted (Fig. S4). For wildfires where daily situation reports were available and at least one structure was reported destroyed (N = 557), the mean lag-time from the day of maximum growth was 5.3 days (median = 2.8 days; mode = 0). It is important to acknowledge that the situation reports may be delayed in their reporting due to the time needed to document structure loss through overflights, remote sensing, or ground-based truthing. To account for the negligible potential of fires in remote areas to affect the built environment, we excluded from the dataset all fires that had not damaged or destroyed any structures. We then applied a regression tree (*75*) to predict the number of structures damaged or destroyed reported across the entire wildfire as a function of maximum fire growth on a single day. The resulting tree was pruned to obtain two classes of fires, i.e., 'very destructive' and 'not very destructive'. Prior to fitting the model, the data were log-transformed to reduce the influence of anomalously large values on the classification. We employed the same methods to estimate thresholds in maximum daily FSR for the 30 states where losses due to wildfires have been reported, and thus also define 'fast fires' at the state level.

The regression tree results indicate (Fig. 2) that fires with a maximum FGR greater than 1,620 ha/day damage or destroy a larger number of structures across CONUS. We choose this threshold as the minimum growth rate for a wildfire to be considered 'fast' at the national scale.

Perhaps unsurprisingly, thresholds vary notably across states for which the models converged (17 states), reflecting differences in local fire behavior and exposure of the built environment (Table S5). Finally, for each EPA ecoregion level IV, we calculated the total number of fast fires and the proportion of fast to total fires in 2001-2020.

IV. Assessing the exposure of the built environment to fast fires

To assess the trends in nearby exposure of the built environment to fast fires, we obtained information from the Historical Settlement Data Compilation of the U.S (HISDAC-US) Built-up Property Records (BUPR) (*42, 76*) which is based on Zillow's Transaction and Assessment Database (ZTRAX). The HISDAC-US database offers a unique source of gridded property information at fine spatial (250 m) and temporal (semi-decade) resolutions (1810-2015). It is worth noting that some uncertainties exist in ZTRAX and are thus propagated to HISDAC-US. For example, HISDAC-US is incomplete in some regions or does not fully account for the number of built structures on the property (*77*). Additionally, the database may not capture areas of significant rebuild following disturbances, which may impact the count of structures in regions with multiple fires or other natural hazards. Despite these limitations, HISDAC-US provides critical information on the location of structures within the built environment at different points in time.

We calculated trends in exposure to fast fires across the contiguous U.S. by overlaying the perimeters of fast fires (1,620 ha/day maximum FGR) between 2001 and 2020 and Historical Built-Up Property Records (BUPR) obtained from HISDAC-US. Specifically, we calculated the annual number of structures within fast fire perimeters, as well as within 1 and 4 km of these fires. We chose to summarize the number of properties exposed to fast fires within 4 km of perimeters due to the risk of long-distance ember throw and home ignition at the fire front (*78*).

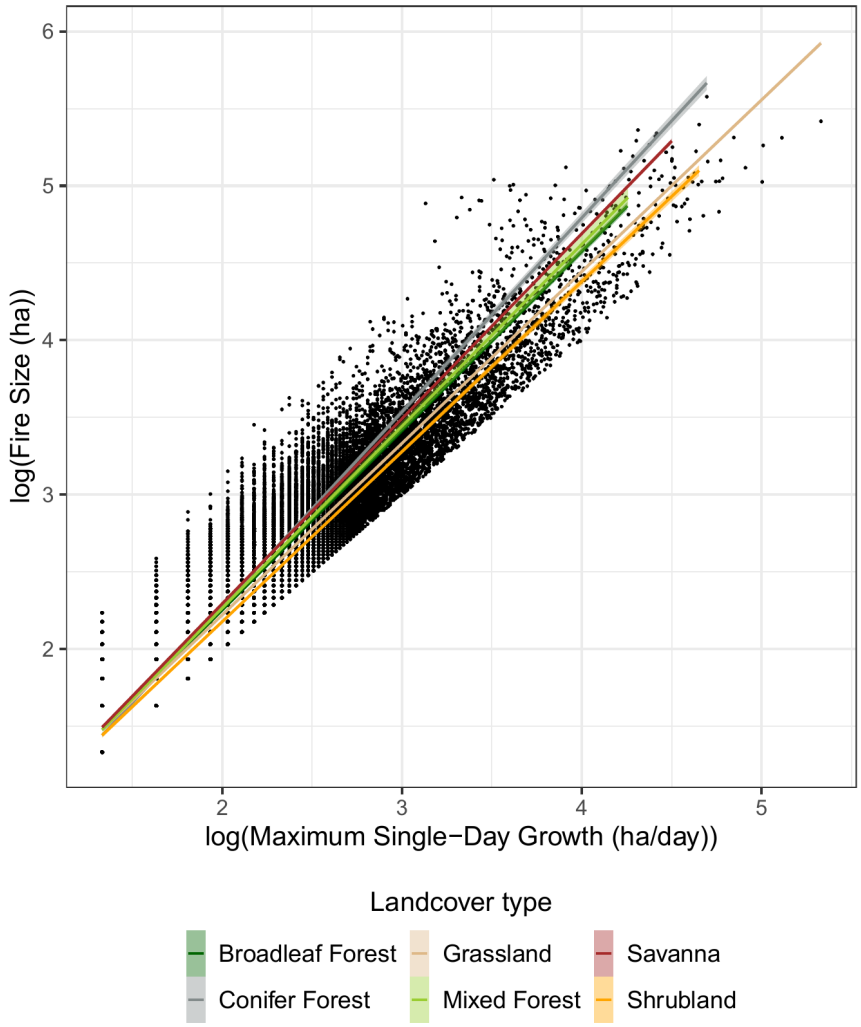

Fig. S1.

Relationship between maximum daily fire growth rate and final fire size in each land cover class in 2000-2020. The log-log transformed variables are strongly correlated, suggesting that they follow a power law (broadleaf forest: coeff = 1.16, adjusted R^2 = 0.9; conifer forest: coeff = 1.26, adjusted R^2 = 0.919; grassland: coeff = 1.11, adjusted R^2 = 0.924; mixed forest: coeff = 1.18, adjusted R^2 = 0.878; savanna: coeff = 1.2, adjusted R^2 = 0.882; shrubland: coeff = 1.1, adjusted R^2 = 0.96).

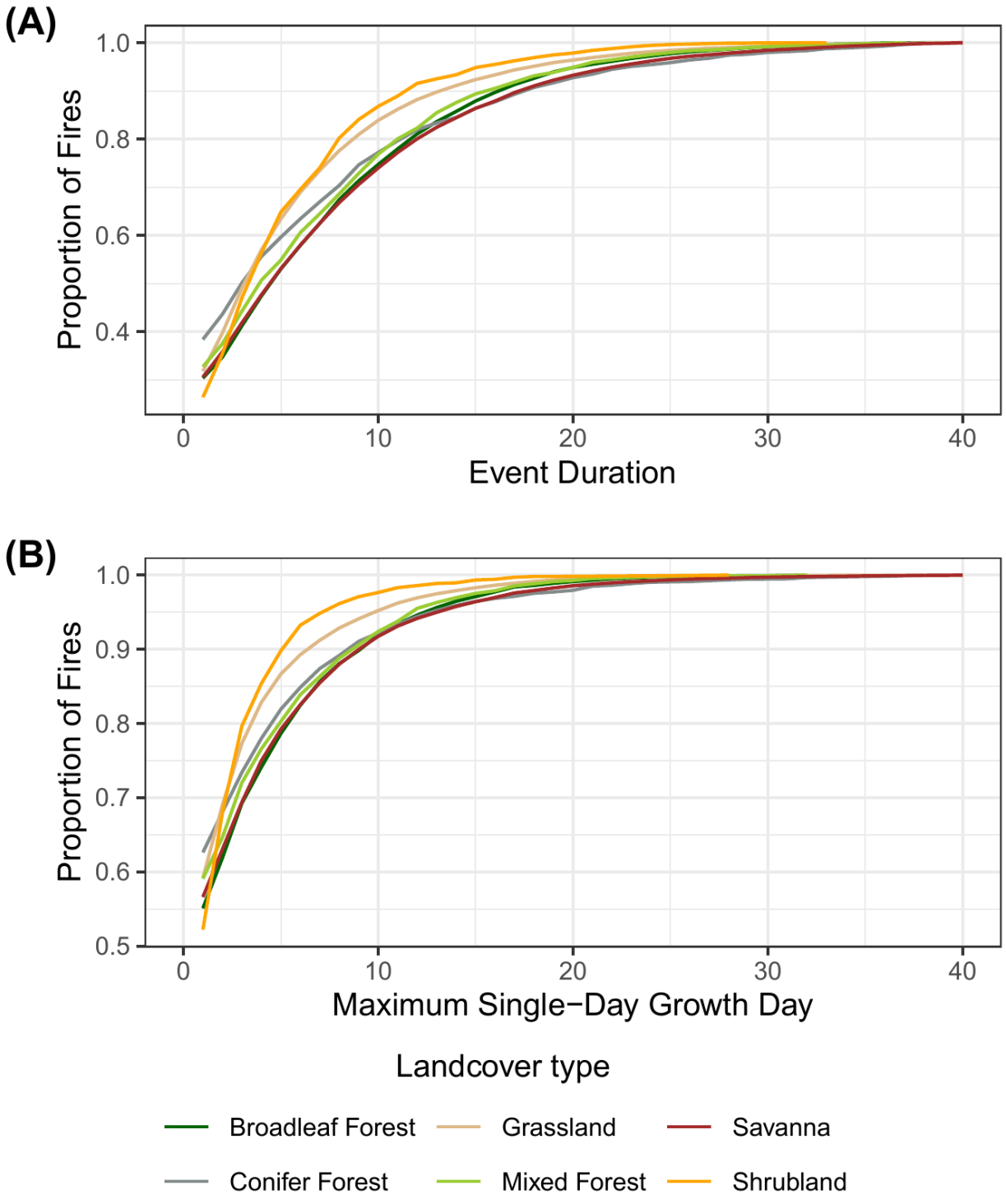

Fig. S2.

Empirical cumulative distribution of (A) fire duration and (B) maximum growth day for all fires analyzed.

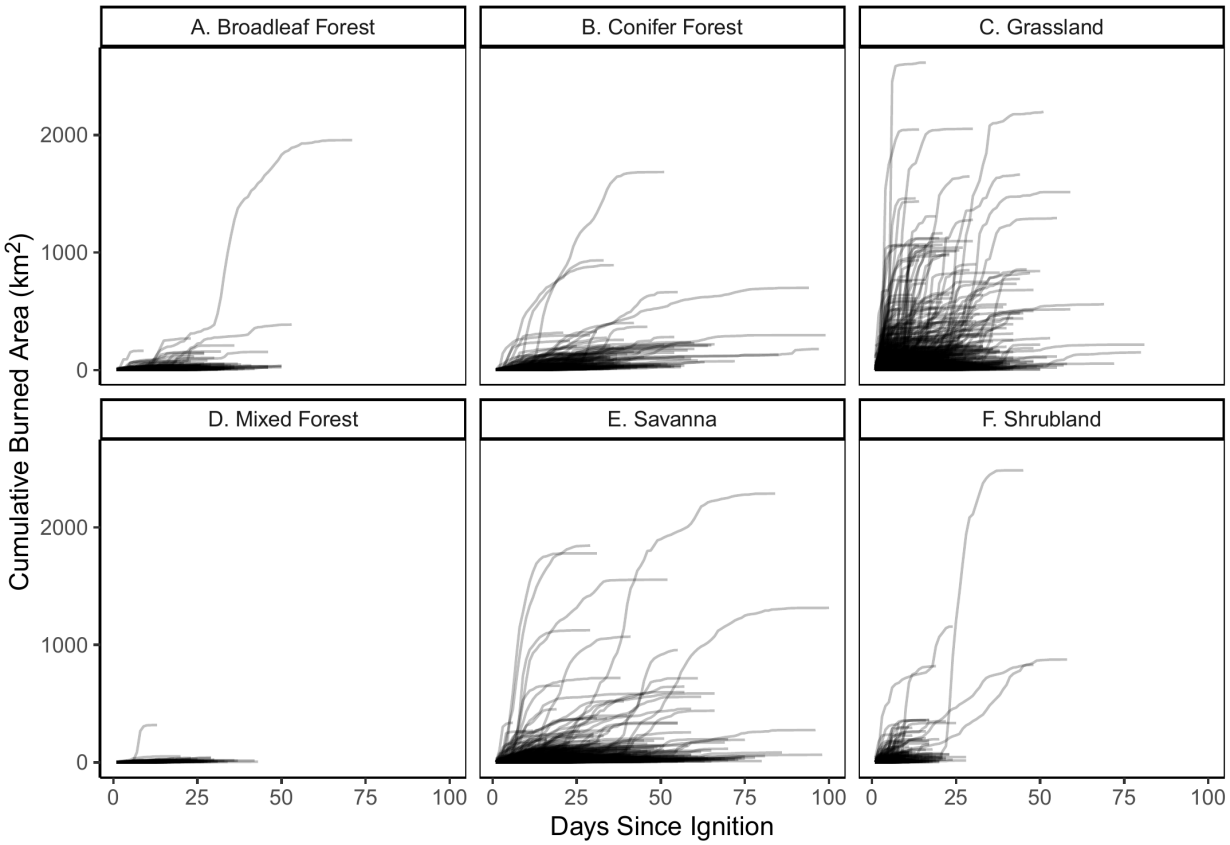

Fig. S3.

Cumulative area burned by the modal land cover type of the event. Most fires that become very large are characterized by a short period of rapid growth. The time period immediately following ignition often has the most fire growth, but the variation in the day of extreme fire growth shows that there is not necessarily one critical period for management. In grasslands and savannas, for many fires almost all of the burned area occurs in a few days. This can occur immediately after ignition, or in many cases pulses of rapid fire growth follow periods of little to no growth.

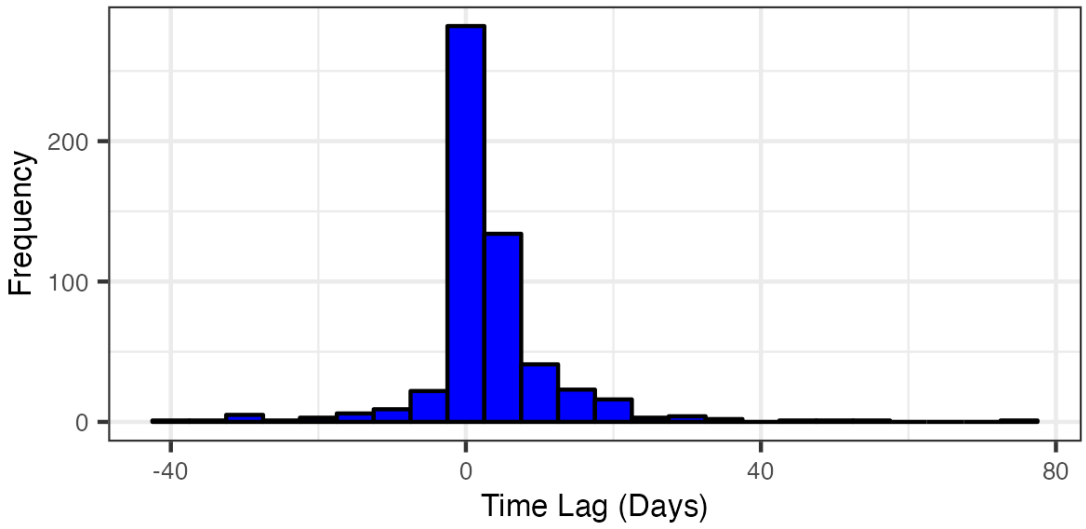

Fig. S4.

Time lag between day of maximum fire growth rate (FGR) and day of maximum structure loss reported. For wildfires where daily situation reports were available and at least one structure was destroyed (N = 557), the median lag-time from the day of maximum growth to the day of maximum structure loss was 2.8 days (mean = 5.3 days; mode = 0 days). While lag times in daily situation reports are expected, there is a clear association between the days of maximum FGR and reported structure loss.

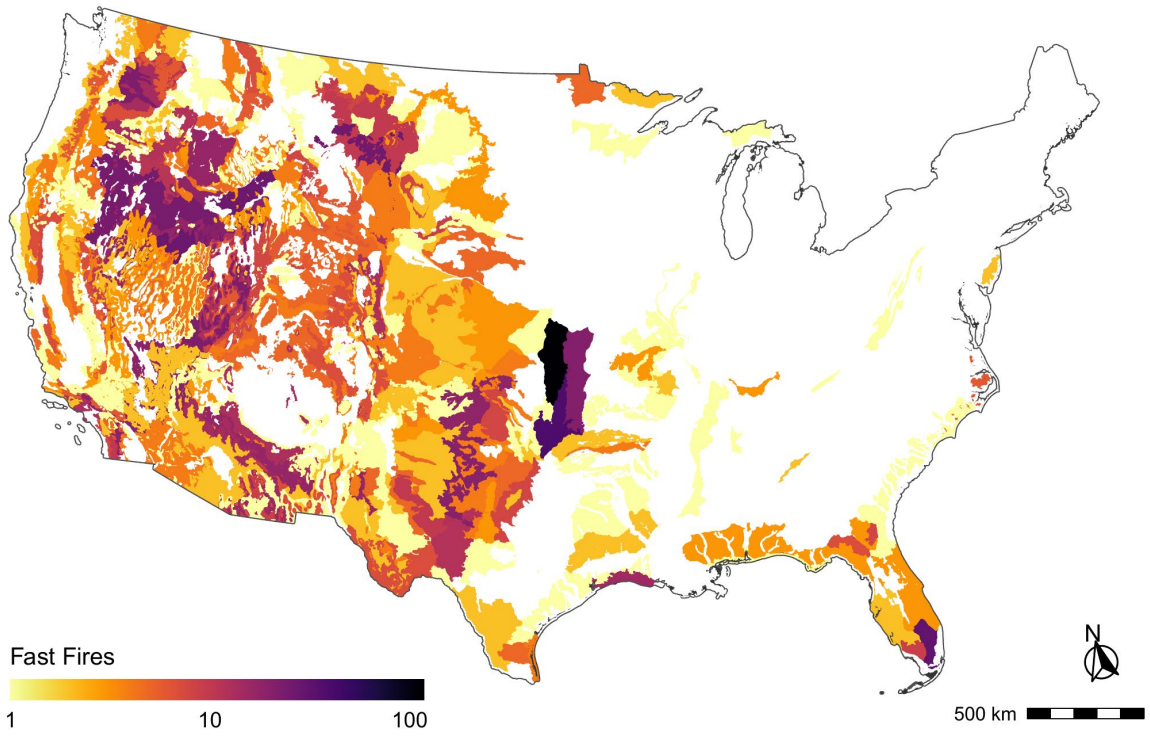

Fig. S5.

Number of fast fires (>1,620ha/day maximum FGR) per EPA ecoregion level IV (2001-2020). Ecoregions that were not affected by fast fires in 2000-2020 are shown in white.

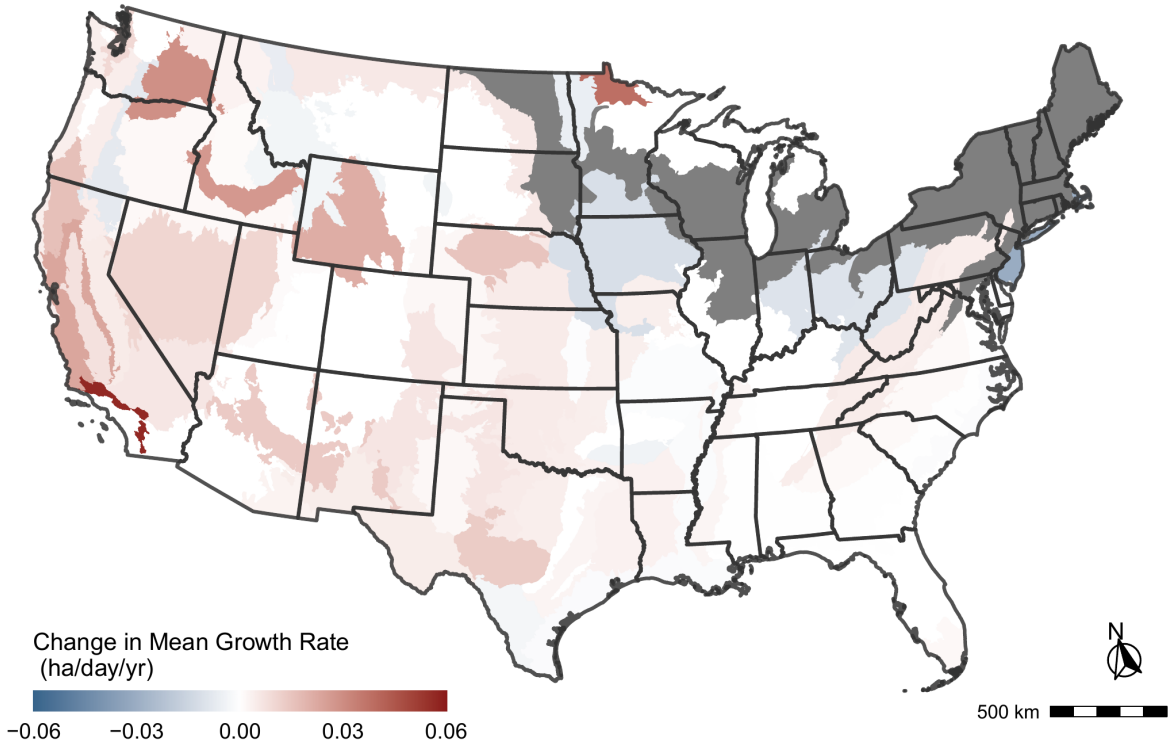

Fig. S6.

Temporal trends in mean fire growth for events longer than four days per EPA ecoregion level IV (2001-2020). Statistically-significant positive and negative regression coefficients ($p < 0.05$) are depicted in warm and cold colors, respectively. Regression coefficients that were not statistically significant from zero (i.e., no significant trend) are shown in white. Ecoregions without sufficient data for the analysis are indicated in gray.

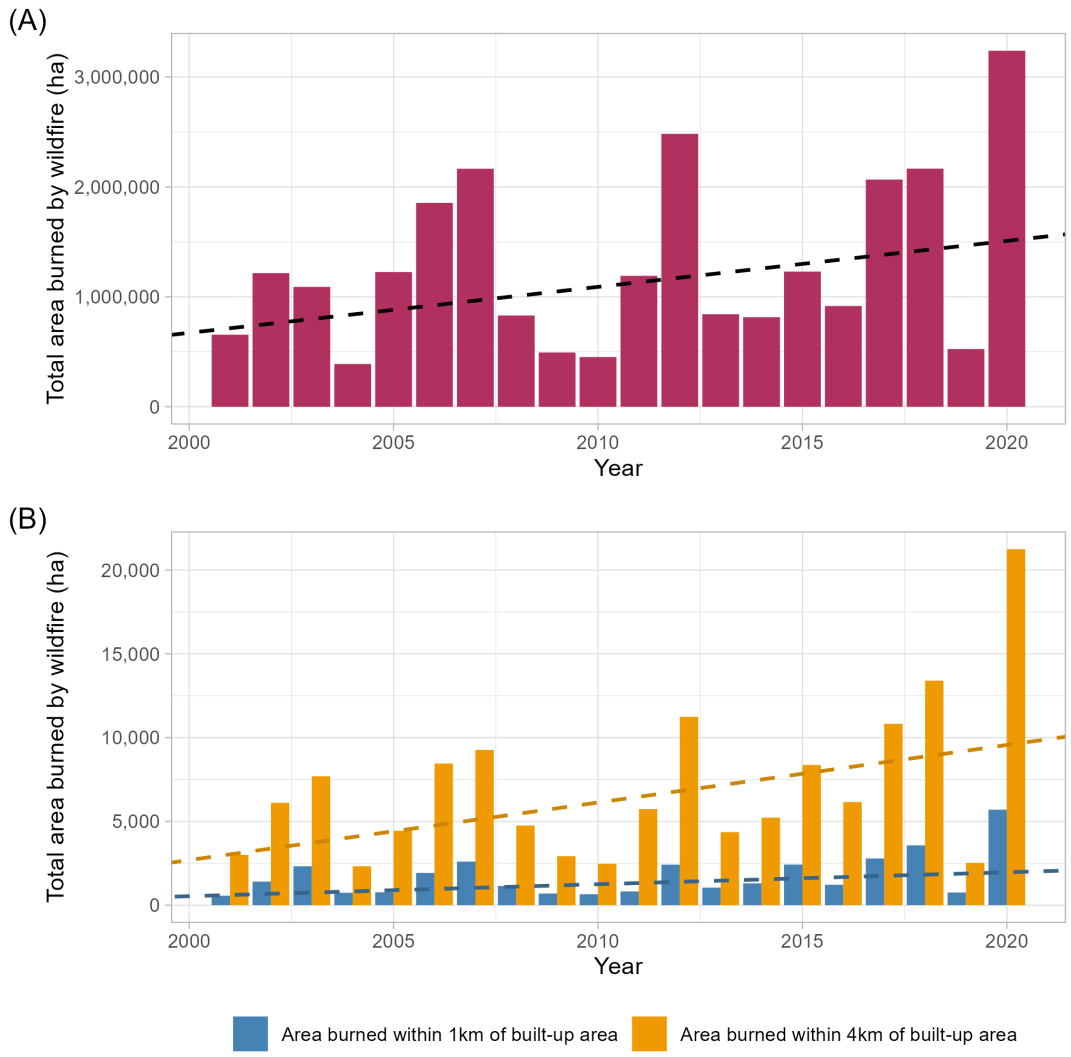

Fig. S7.

Increase in western United States annual burned area overall and near built-up areas, 2001-2020. (A) Annual burned area from wildfires in the western U.S. based on FIRED data for 2001-2020. Trend line determined by Theil-Sen regression, coefficient = 41,807 ha/year ($p < 0.01$). Trend burned area as a percentage of 2001 grew to 211% in 2020. **(B)** Annual burned area within 1 and 4 km of built-up areas in the western U.S., as determined by BUPR layers in 2000, 2005, 2010, 2015, and 2020. Trend lines determined by Theil-Sen regression. Trend for burned area within 1 km of built-up areas, coefficient = 71 ha/year ($p < 0.0001$); as a percentage of 2001, grew to 323% in 2020. Trend for burned area within 4 km of built-up areas, coefficient = 343 ha/year ($p < 0.0001$); as a percentage of 2001, grew to 315% in 2020. Near-built-up proportion of total burned area in the western U.S. ranges from 0.06% - 0.21% annually for 1 km and from 0.36% - 0.71% annually for 4 km. Increases in the near-built-up proportion of total annual burned area in the western U.S. are significant ($p < 0.01$), but marginal (coefficients = 0.006% / year (1 km) and 0.003% / year (4 km)).

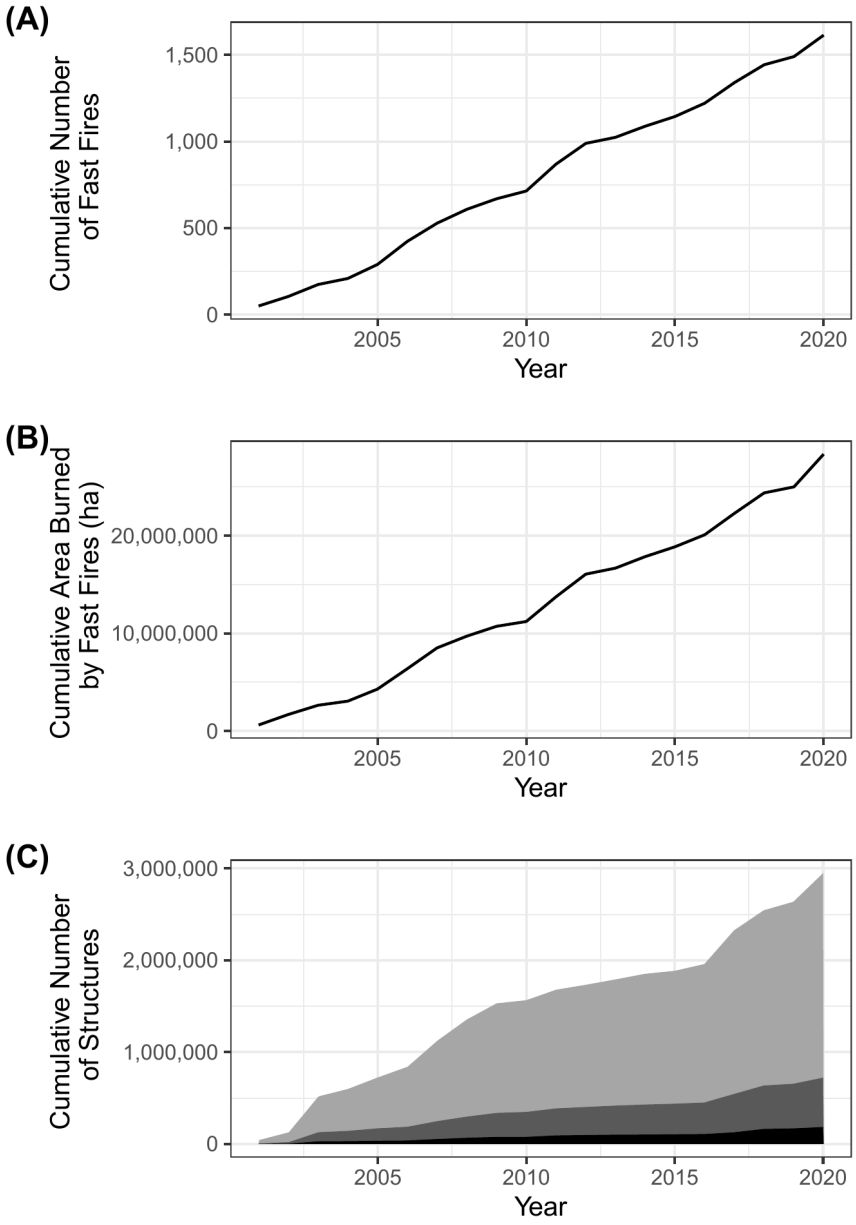

Fig. S8.

Exposure to fast fires (>1,620 ha/day) in 2001-2020. (A) Cumulative number of fast fires. **(B)** Cumulative area affected by fast fires. **(C)** Trends in the cumulative number of structures within the perimeters of fast fires (black), within 1 km of the perimeters of fast fires (dark gray), and within 4 km of the perimeters of fast fires (light gray).

Table S1. (separate file)

Ecoregion Fire Characteristic Summaries, 2001-2020. Ecoregions marked with "*" are defined by EPA Level I Ecoregions. Within the contiguous United States 60,012 fires were included for analysis, of which 1,616 (2.69%) were Fast. The mean of the single day maximum fire growth rate was 297.9 ha/day. Reported characteristics include: *Median Single Day Maximum Fire Growth Rate (ha / day), Mean Single Day Maximum Fire Growth Rate (ha / day), Maximum Single Day Maximum Fire Growth Rate (ha / day), Median Fire Growth Rate (ha / day), Mean Fire Growth Rate (ha / day), Median Fire Duration (days), Mean Fire Duration (days), Median Fire Size (ha), Mean Fire Size (ha), Total Number of Fires, Number of Fast Fires, and Fast Fires Percentage of Total Fires (%).*

Table S2. (separate file)

Statistics for area burned during the day of maximum fire growth for land cover types within ecoregions, 2001-2020. Across 60,012 events within the contiguous United States, over 47 million hectares were burned between 2001 and 2020. Of this total area burned, 37.9% was burned during the day of maximum fire growth for each event. The 'Non-vegetated' land cover type includes >60% barren, permanent wetlands, and >60% snow/ice. Statistics reported include: *Number of Fire Events, Total Area Burned (ha), Area Burned During Day of Maximum Growth across all Events (ha), Area Burned During Day of Maximum Growth for the Fastest Event (ha), Percent of Total Area Burned During Day of Maximum Growth across all Events (%), Percent of Total Area Burned During Day of Maximum Growth for the Fastest Event (%), Average Event Area Burned During Day of Maximum Growth (ha)*

Table S3. (separate file)

Land cover Fire Characteristic Summaries for CONUS and the western United States, 2001-2020. Within the contiguous United States 60,012 fires were included for analysis, of which 1,616 (2.69%) were Fast. The mean of the single day maximum fire growth rate was 297.9 ha/day. Reported characteristics include: *Median Single Day Maximum Fire Growth Rate (ha / day), Mean Single Day Maximum Fire Growth Rate (ha / day), Maximum Single Day Maximum Fire Growth Rate (ha / day), Median Fire Growth Rate (ha / day), Mean Fire Growth Rate (ha / day), Median Fire Duration (days), Mean Fire Duration (days), Median Fire Size (ha), Mean Fire Size (ha), Total Number of Fires, Number of Fast Fires, and Fast Fires Percentage of Total Fires (%).*

Table S4. (separate file)

Top 100 fastest growing fires across CONUS (2001-2020). Summary of statistics from the top 100 fastest fires from FIRED linked to their associated incident command report (*44*). For only one of the top 100 fastest fires, there was not a one-to-one match between a FIRED perimeter and associated incident command report so we do not report the statistics from that event. The top 100 fastest fires accrued an estimated $3.37B in suppression costs, exposed 905,781 properties (within 4 km) and destroyed structures. Of the 100 fastest fires, 68 occurred primarily in grassland vegetation types (>50% grassland in burned area). Statistics reported include: *Incident Name, Ignition Year, State, Fire Size (ha), Max Fire Growth (ha/day), Fire Duration (days), Cost ($), Properties Exposed (within 4km), Structures Destroyed, Total Aerial Units, Total Personnel, and Dominant Vegetation Type.*

Table S5. (separate file)

Thresholds in maximum daily FGR for the states in the contiguous United States where losses to wildfires have been reported. These thresholds were used to define 'fast fires' at the state level. Statistics reported include: *State, Total number of fires that threatened any structure, Total number of structures damaged or destroyed, Maximum daily fire growth rate (ha/day), Fast fire threshold (ha/day), Number of fast fires, and Number of structures damaged or destroyed by fast fires.* 'No convergence' means the model did not have enough data.

Table S6. (separate file)

Fire characteristic trend coefficients and p-values by EPA Level III Ecoregions. P-value significance symbols: 0.05 (*), 0.01 (**), 0.001 (***). Trend coefficients and p-values reported include: *Single Day Maximum Fire Growth Rate Theil-Sen Coefficient (ha/day/year), Single Day Maximum Fire Growth Rate P-value, Single Day Maximum Fire Growth Rate P-value Significance, Fire Duration Theil-Sen Coefficient (day/year), Fire Duration P-value, Fire Duration P-value Significance, Simple Fire Spread Rate Theil-Sen Coefficient (ha/day/year), Simple Fire Spread Rate P-value, and Simple Fire Spread Rate P-value Significance.*

Region	Mean Increase in Fire Growth Rate (ha/day/year)	Median Increase in Fire Growth Rate (ha/day/year)	Bootstrapped Increase in Fire Mean Growth Rate (ha/day/year)	Bootstrapped Increase in Fire Median Growth Rate (ha/day/year)	Total Increase in Fire Growth Rate Across 19 Years (ha/day)	Mean Fire Growth Rate Across 20 Years (ha/day)	Growth Rate Increase as a Percentage of 20-year Mean Fire Growth (%)
California	4.24 +/- 0.38	2.39 +/- 0.28	4.3 +/- 0.4	2.25 +/- 0.31	80.56	124.28	64.82
West	2.14 +/- 0.12	0 +/- 0.75	1.0 +/- 0.26	0 +/- 0.88	40.66	159.33	25.52

Table S7.

Temporal changes in fire growth rate for California and the western United States. For each region we calculated the mean and median (+/- standard errors) of Theil-Sen regression coefficients of all sub-ecoregions, in addition to the bootstrapped estimation of the Theil-Sen coefficient.

Region	Mean maximum fire growth rate in 2001 (ha/day)	Median maximum fire growth rate in 2001 (ha/day)	Mean maximum fire growth rate in 2020 (ha/day)	Median maximum fire growth rate in 2020 (ha/day)	Mean maximum fire growth rate in 2020 as a percentage of mean maximum fire growth rate in 2001 (%)	Median maximum fire growth rate in 2020 as a percentage of median maximum fire growth rate in 2001 (%)
California	1,175	515	4,676	1,009	397.96	195.92
West	1,025	258	2,557	451	249.46	174.81

Table S8.

Percent increases in maximum fire growth rate between 2001 and 2020 for California and the western United States. Values are calculated from raw data and exclude croplands.